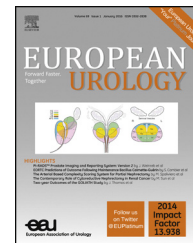


available at www.sciencedirect.com
journal homepage: www.europeanurology.com



European Association of Urology



Platinum Priority – Prostate Cancer

Editorial by XXX on pp. x–y of this issue

Comprehensive Drug Testing of Patient-derived Conditionally Reprogrammed Cells from Castration-resistant Prostate Cancer

Khalid Saeed^a, Vesa Rahkama^a, Samuli Eldfors^a, Dmitry Bychkov^a, John Patrick Mpindi^a, Bhagwan Yadav^a, Lassi Paavolainen^a, Tero Aittokallio^a, Caroline Heckman^a, Krister Wennerberg^a, Donna M. Peehl^b, Peter Horvath^{a,c}, Tuomas Mirtti^{a,d}, Antti Rannikko^e, Olli Kallioniemi^{a,†}, Päivi Östling^{a,†}, Taija M. af Hällström^{a,†,*}

^aInstitute for Molecular Medicine Finland, University of Helsinki, Helsinki, Finland; ^bDepartment of Urology, Stanford University School of Medicine, Stanford, CA, USA; ^cSynthetic and System Biology Unit, Biological Research Center, Szeged, Hungary; ^dDepartment of Pathology, HUSLAB, Helsinki University Hospital, Helsinki, Finland; ^eDepartment of Urology, Helsinki University Hospital, Helsinki, Finland

Article info

Article history:

Accepted April 15, 2016

Associate Editor:

James Catto

Keywords:

Castration-resistant prostate cancer
Drug sensitivity testing
Navitoclax
Patient-derived cultures
Reprogrammed cells

Abstract

Background: Technology development to enable the culture of human prostate cancer (PCa) progenitor cells is required for the identification of new, potentially curative therapies for PCa.

Objective: We established and characterized patient-derived conditionally reprogrammed cells (CRCs) to assess their biological properties and to apply these to test the efficacies of drugs.

Design, setting, and participants: CRCs were established from seven patient samples with disease ranging from primary PCa to advanced castration-resistant PCa (CRPC). The CRCs were characterized by genomic, transcriptomic, protein expression, and drug profiling.

Outcome measurements and statistical analysis: The phenotypic quantification of the CRCs was done based on immunostaining followed by image analysis with Advanced Cell Classifier using Random Forest supervised machine learning. Copy number aberrations (CNAs) were called from whole-exome sequencing and transcriptomics using in-house pipelines. Dose-response measurements were used to generate multiparameter drug sensitivity scores using R-statistical language.

Results and limitations: We generated six benign CRC cultures which all had an androgen receptor-negative, basal/transit-amplifying phenotype with few CNAs. In three-dimensional cell culture, these cells could re-express the androgen receptor. The CRCs from a CRPC patient (HUB.5) displayed multiple CNAs, many of which were shared with the parental tumor. We carried out high-throughput drug-response studies with 306 emerging and clinical cancer drugs. Using the benign CRCs as controls, we identified the Bcl-2 family inhibitor navitoclax as the most potent cancer-specific drug for the CRCs from a CRPC patient. Other drug efficacies included taxanes, mepacrine, and retinoids.

Conclusions: Comprehensive cancer pharmacopeia-wide drug testing of CRCs from a CRPC patient highlighted both known and novel drug sensitivities in PCa, including navitoclax, which is currently being tested in clinical trials of CRPC.

Patient summary: We describe an approach to generate patient-derived cancer cells from advanced prostate cancer and apply such cells to discover drugs that could be applied in clinical trials for castration-resistant prostate cancer.

© 2016 European Association of Urology. Published by Elsevier B.V. This is an open access article under the CC BY-NC-ND license (<http://creativecommons.org/licenses/by-nc-nd/4.0/>).

† These authors are senior team members.

* Corresponding author. Institute for Molecular Medicine Finland, University of Helsinki, Haartmaninkatu 8, Helsinki FI-00140, Finland. Tel. +358-400-520088; Fax: +358-294125737.
E-mail address: taija.afhallstrom@helsinki.fi (T.M. af Hällström).

<http://dx.doi.org/10.1016/j.eururo.2016.04.019>

0302-2838/© 2016 European Association of Urology. Published by Elsevier B.V. This is an open access article under the CC BY-NC-ND license (<http://creativecommons.org/licenses/by-nc-nd/4.0/>).

Please cite this article in press as: Saeed K, et al. Comprehensive Drug Testing of Patient-derived Conditionally Reprogrammed Cells from Castration-resistant Prostate Cancer. Eur Urol (2016), <http://dx.doi.org/10.1016/j.eururo.2016.04.019>

1. Introduction

Prostate cancer (PCa) is the most common noncutaneous malignancy and the second leading cause of cancer deaths in men. Localized PCa is treated with surgery, radiation, or surveillance, whereas androgen-deprivation therapy (castration) is the standard of care for advanced PCa [1,2]. Typically, most patients respond to castration as demonstrated by falling prostate-specific antigen (PSA) and quick relief of symptoms [3]. Ultimately, the disease progresses (rising PSA and/or growth of metastases) to a state called castration-resistant prostate cancer (CRPC) [4]. At this stage, alternative treatments available include novel drugs such as abiraterone and enzalutamide, radium-223 (a radiopharmaceutical), and cytotoxic drugs such as docetaxel and cabazitaxel [5–11]. However, eventually the cancer cells become resistant to hormonal and radiopharmaceutical treatments and the currently available cytotoxic drugs.

The prostate gland consists of glandular epithelium in which five cell types have been identified: basal, transit-amplifying (TA), luminal, neuroendocrine, and stem cells [12]. Basal cells are androgen independent and can be characterized by their expression of cytokeratins (CK)-5 and CK14. In contrast, luminal epithelial cells are androgen dependent and can be identified by CK18, androgen receptor (AR), and PSA expression. The TA cells are thought to migrate from the basal to the luminal layer as they differentiate and express a combination of markers common to both cell types [12–14]. It has been suggested that PCa may arise from the AR-negative, androgen-independent basal stem cells, which are able to survive during androgen deprivation therapy [12]. Furthermore, cells expressing low amounts of AR and PSA within the prostate have been suggested to exhibit long-term tumor-propagating capacity and are not vulnerable to stress caused by the androgen deprivation [15].

Establishment and maintenance of long-term ex vivo cultures directly from patient-derived prostate tumor tissue samples has been very challenging, but this is starting to change due to recent breakthroughs in two dimensional (2D) and 3D cell culture technologies [16–18]. These new primary culture technologies consist of either conditionally reprogrammed cells (CRCs) cocultured as monolayers (in 2D) with feeder cells (irradiated-3T3 mouse fibroblasts) in the presence of a Rho-associated protein kinase inhibitor (ROCKi) or of patient-derived spheroids or organoids (in 3D). Importantly, these models are not established through xenografting or exogenous gene transfer and they could become critically important in understanding the disease and identifying new therapeutic agents for PCa.

Here, we generated patient-derived CRCs of PCa from castration-naïve PCa to CRPC as well as from benign tissues as controls. We characterized these CRCs with genomic, transcriptomic, and protein expression profiling and compared them with the parental tissues from which they were isolated. We then performed comprehensive drug sensitivity testing with 306 oncology drugs to identify clinical and emerging oncology drugs that could be effective for PCa-derived CRCs [19,20].

2. Materials and methods

2.1. Tissue processing and establishment of CRCs

Prostate tissue was collected from seven patients undergoing prostatectomy, transurethral resection of the prostate, or ultrasound-guided needle biopsy at Helsinki University Hospital. Samples were obtained from patients participating with informed consent in the Urological Biobank Initiative (Helsinki Urological Biobank; HUB). With radical prostatectomy patient samples, a cylinder shaped core of prostate tissue (8-mm diameter) was cored out of the peripheral dorsal region of the prostate and tissue was processed as illustrated in Figure 1. Primary cells for the establishment of CRCs were isolated from the middle section of the core. The ratio of benign and malignant cells in the parental tissue was evaluated from tissue sections adjacent to the section used for CRC establishment using hematoxylin and eosin staining (Supplementary Table 1). The inclusion criteria for the patient samples included the ratio of benign and malignant cells in the tissue; therefore, only tissues without cancer cells were used for benign CRC establishment and tissues with less than 15% of contaminating benign cells were used for cancer CRC establishment. The methodology is described in more detail in the supplementary material.

2.2. Copy number aberration analysis

Genomic DNA was extracted from parental tissues, CRCs, and germline control blood cells using the DNeasy Blood & Tissue kit (Qiagen, Hilden, Germany). The methodology and analysis pipeline are described in the supplementary material.

2.3. Immunohistochemistry, immunofluorescence labeling, and image analysis

Immunohistochemistry (IHC) and immunofluorescence (IF) labeling were performed according to standard operating procedures. Phenotypic and apoptosis quantification based on IF labeling coupled with supervised machine learning image analysis were developed in-house, as described in the supplementary material.

2.4. Drug sensitivity testing

The CRCs established from the patient samples were cultured for 3–7 wk and used for drug testing with 306 clinical (Food and Drug Administration and/or European Medicines Agency-approved) and emerging oncology drugs as described in Pemovska et al [19]. Briefly, cells were exposed to drugs in five different concentrations for 72 h. The viability of the CRCs was measured with CellTiter-Glo (CTG, Promega, Madison, WI, USA). To determine whether the ROCK inhibitor (Y-27632) would affect the sensitivity profile, we performed replicate screens with and without Y-27632 for HUB.1, HUB.2, HUB.3, and HUB.7 (Supplementary Fig. 3). The comparison of the drug sensitivity score (DSS) between the replicate screens showed strong correlation ($R^2 > 0.90$, $p < 0.0001$), and thus to maintain an optimal proliferative state of the CRCs (Fig. 1D). Y-27632 was present in all the subsequent tests.

2.5. Statistical analysis

The dose-response percent inhibition data points were fitted into a four-parameter logistic model to calculate IC50, slope, top, and lower asymptotes. These parameters were used to quantify the drug response, using a multiparameter area under the curve sensitivity calculation called the DSS. The DSS was calculated for each drug and compared between the averaged controls and CRCs to obtain patient specific DSS

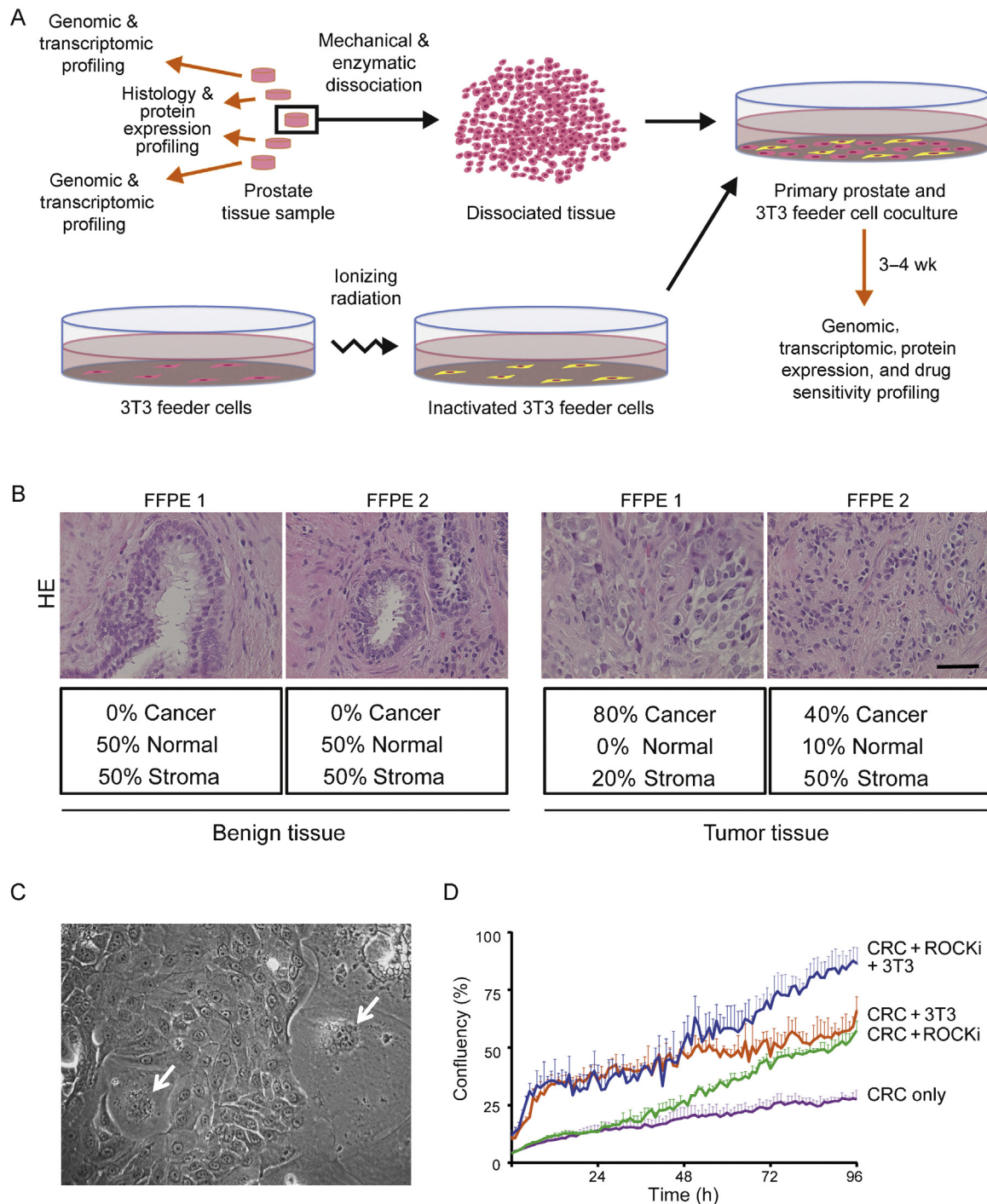


Fig. 1 – Diagram of tissue processing and establishment of conditionally reprogrammed cells (CRCs). (A) The peripheral tissue pieces of the prostate tissue sample were snap-frozen and used for genomic and transcriptomic profiling. Adjacent tissue pieces were fixed in 10% buffered formalin and used for histological evaluation (hematoxylin and eosin; HE) and protein expression profiling by immunohistochemistry. The CRC cultures were initiated from the middle section of the prostate tissue sample. The tissue was mechanically and enzymatically dissociated and cocultured with inactivated 3T3 feeder cells in Rho-associated protein kinase inhibitor (ROCKi; Y-27632) supplemented medium until entering the genomic, transcriptomic, protein expression, and drug sensitivity profiling. (B) A representation of HE based histological evaluation of parental benign tissue and tumor tissue used for determining the histological origin of CRCs. The representative images were obtained using 40× objective and the scale bar indicates 100 μm. (C) A light microscope image of CRCs and 3T3 feeder cells (white arrows). The image was taken with 20× objective. (D) A growth curve of CRCs grown for 96 h with both feeder cells (3T3) and ROCKi in F-medium (blue line), with feeder cells only in F-medium (orange line), with ROCKi only in F-medium (green line), and with F-medium without feeders and ROCKi (purple line). Error bars indicate the standard deviation of at least triplicate wells. FFPE = formalin-fixed, paraffin-embedded.

(selective DSS) as previously described [20]. Pearson correlation coefficient was used to assess the significance of correlations displayed in the XY plots across drug sensitivity and GraphPad Prism 6 (GraphPad Software Inc., La Jolla, CA, USA) was used to generate these plots as well as the combined dose-response curve fits illustrated in Supplementary Figure 4A. The R statistical programming language and the heatmap function from Heatplus Bioconductor package (v.2.15.3, <http://www.r-project.org/>) were used to generate the selective DSS heatmap. Clustering of the drug sensitivity profiles across the samples was done with unsupervised hierarchical clustering based on the Ward-linkage method and Spearman's rank as the distance metric.

3. Results

3.1. Prostate tissue processing and establishment of the CRC cultures

For this study, we selected seven patients whose disease ranged from benign to early prostate cancer and CRPC (HUB.1–7; Table 1). Based on the histological evaluation, altogether seven tumor and two benign samples were used for the establishment of CRCs (Table 1, Fig. 1A and 1B, Supplementary Table 1). The CRCs were generated through coculturing of freshly isolated patient cells and feeder cells in culture medium supplemented with ROCKi [16]. In this system patient-derived CRCs grow in colonies typical of epithelial cells (Fig. 1C). The optimal growth conditions for the CRCs were tested in live phase contrast imaging in four different conditions: (1) with both feeder cells and ROCKi, (2) with feeder cells only, (3) with ROCKi only, and (4) without feeder cells and ROCKi. The results show that both feeder cells and ROCKi were necessary for the optimal cell growth (Fig. 1D). Seven out of nine (78%) attempts to start CRC cultures were successful. The CRCs were characterized with genomic, transcriptomic, and protein expression profiling, and compared with the parental tissue from which the benign and cancer cells were isolated (Supplementary Table 2).

3.2. Molecular characteristics of the CRCs

To define and quantify the phenotypic variation in the CRCs, we performed IF labeling of the cells coupled with supervised machine learning image analysis using five classifiers: (1) cell nuclei, (2) basal cells (CK5/p63 positive), (3) luminal cells (CK18 positive), and (4) TA cells (CK5/p63 and CK18 positive), as well as (5) other types. We observed

basal cell markers p63/CK5 and luminal cell marker CK18 being expressed either alone or simultaneously (TA phenotype) in all CRCs (Fig. 2A and 2B). Five out of seven (71%) CRCs were dominated by the TA phenotype whereas in two CRCs (HUB.1 and HUB.5), the basal phenotype was more prominent. Additionally, HUB.3.CC displayed a strong luminal population (45%). We confirmed the expression of these cell type-specific markers using western blotting and IHC of formalin-fixed, paraffin-embedded samples from the corresponding tissue and CRCs (Fig. 2C and 2D, Supplementary Fig. 1).

All the CRCs were found to be AR and PSA negative in contrast to their parental tissue (Fig. 2C and 2D, Supplementary Fig. 1), which was also confirmed by RNA-sequencing and quantitative polymerase chain reaction (data not shown). We were able to restore AR expression in HUB.1 CRCs when grown in 3D spheroid culture (Fig. 2E), whereas the CRPC-derived HUB.5 CRCs were not able to grow as spheroids (data not shown).

Genomic analysis was performed to identify cancer-specific copy number aberrations (CNAs) in the CRCs and compare these with the CNAs found in the parental tissue. Most of the CRCs had no shared CNAs with the matching parental tissue, suggesting that they represented benign cells (Supplementary Fig. 2A). In contrast, HUB.5 CRCs shared the same cancer-specific deletions at chromosomes 1p and 16p with their parental tumor tissue (Fig. 2F, Supplementary Fig. 2B). A full list of HUB.5 CRC-specific somatic mutations is provided in Supplementary Table 3. Thus, the HUB.5 CRC model appears to be a bona fide PCa CRC model established in this study.

3.3. Comprehensive oncology drug testing in the CRPC-derived HUB.5 CRCs

To identify vulnerabilities of HUB.5 CRCs towards oncology drugs we performed drug testing using 306 oncology drugs in five different concentrations and measured cell viability after 72 h of drug exposure [19,20] (Supplementary Table 4). To obtain a HUB.5 cancer-selective sensitivity profile, we used two sets of controls, the first set with the mean of two CRC models derived from benign prostate tissue (HUB.2.BC and HUB.3.BC) and the second set with the mean of all other CRCs established in this study, except for HUB.5. The results from both sets of controls showed cancer-specific DSS for HUB.5 for several drugs that

Table 1 – Patient characteristics and initiated conditionally reprogrammed cells (CRC)

Patient	Gleason score	PSA (ng/ml)	TNM	Previous treatments	Tissue source	Benign CRC	Cancer CRC
HUB.1	4 + 5 = 9 (70%)	15.5	pT3bN0M0	–	RALP	–	1
HUB.2	4 + 5 = 9 (30%)	7.53	pT3aN0M0	–	RALP	1	1
HUB.3	4 + 5 = 9 (10%)	8.54	pT3N1M0	–	RALP	1	1
HUB.4	5 + 4 = 9 (90%)	92	cT3N0M0	Orchiectomy, bicalutamide	TURP	–	1
HUB.5	5 + 4 = 9 (80%)	1.67	cT4N1M1	LH-RH-agonist, bicalutamide, docetaxel, abiraterone	TURP	–	1
HUB.6	3 + 4 = 7 (24%)	4.06	cT3N0M0	External radiation and bicalutamide	Needle biopsy	–	1
HUB.7	4 + 4 = 8 (NA)	2.96	cT4N1M1	Orchiectomy, palliative TURP	Needle biopsy	–	1

HUB = Helsinki Urological Biobank; LH-RH-agonist = luteinizing hormone-releasing hormone agonist; NA = not applicable; PSA = prostate-specific antigen; RALP = robotic-assisted laparoscopic prostatectomy; TURP = transurethral resection of the prostate.

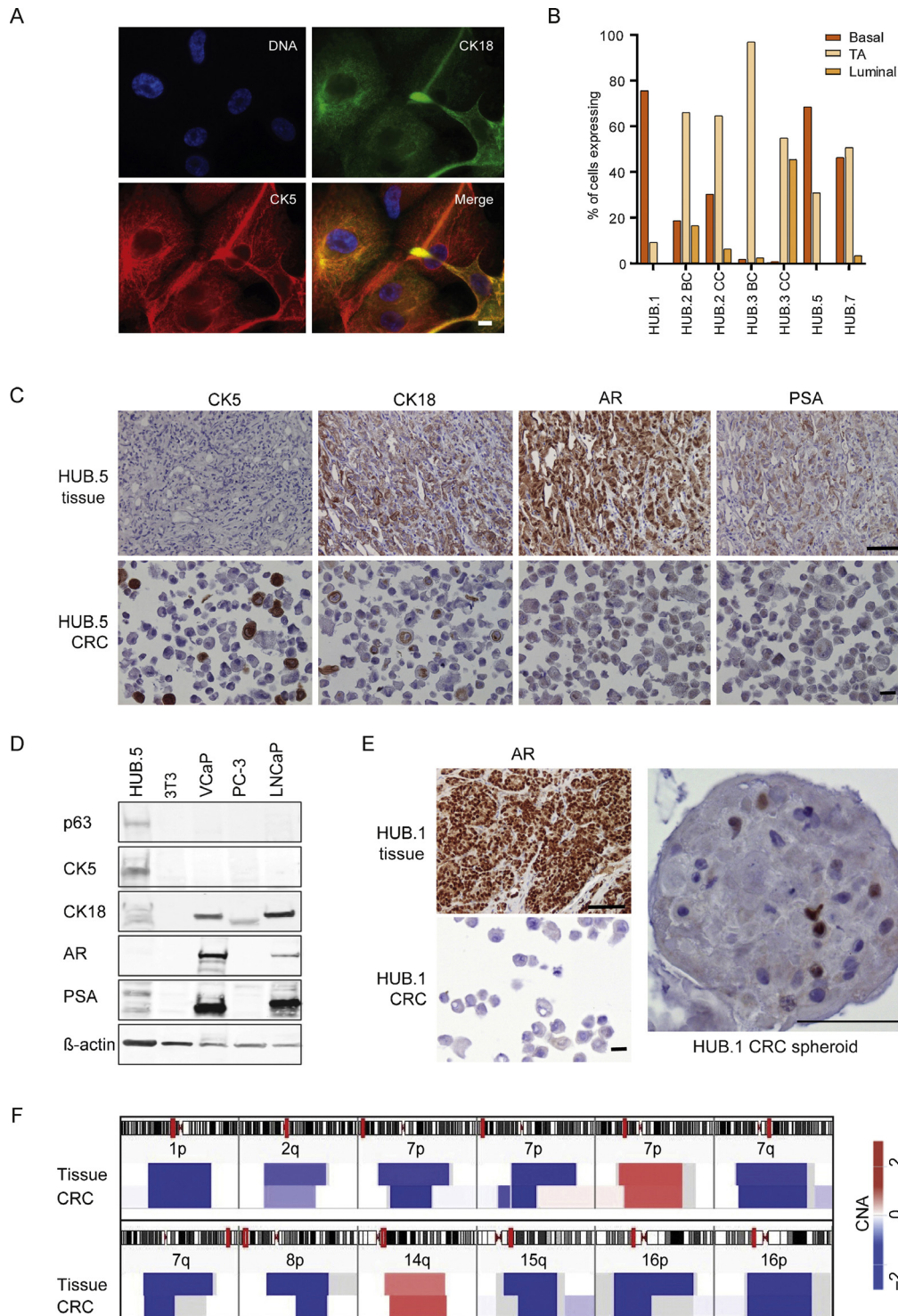


Fig. 2 – Characterization of conditionally reprogrammed cells (CRCs) and the parental tissue. (A) Representative immunofluorescence images of the CRCs showing phenotypic classifiers for basal (cytokeratin [CK]-5; red), transit-amplifying (TA; CK5 and CK18; yellow), and luminal cells (CK18; green). The nuclei were counterstained with Hoechst 33342 for DNA. The images were taken with 60× objective and the scale bar indicates 10 μm. **(B)** Phenotypic quantification of basal, TA, and luminal populations of the given patient-derived samples excluding mitotic, abnormal, and feeder cells shown in percentages. A total of 145 to 566 cells were analyzed per sample. BC and CC indicates CRCs isolated from benign areas and malignant areas respectively. **(C)** Immunohistochemistry staining of castration-resistant prostate cancer HUB.5 tissue and CRCs with the indicated markers. Images of representative fields were captured at 20× (tissue) and 40× (cytoblock) magnification and the scale bars indicate 100 μm (tissue) and 20 μm (cytoblock). **(D)** Western blotting analysis of HUB.5 CRCs and control cell lines with the following markers: p63, CK5, CK18, androgen receptor (AR), prostate-specific antigen (PSA), and actin. **(E)** Immunohistochemistry staining of AR expression in HUB.1 tissue, CRCs, and spheroids. The scale bars indicate 100 μm (tissue), 20 μm (cytoblock), and 100 μm (spheroid). **(F)** Visualization of the HUB.5 parental tissue and CRCs showed similar copy number aberrations (CNAs) at chromosomes 1p, 2q, 7p, 7q, 8p, 14q, 15q, and 16p with exact breakpoint matches at chromosomes 1p and 16p. Red color represents copy number gains and blue deletions.

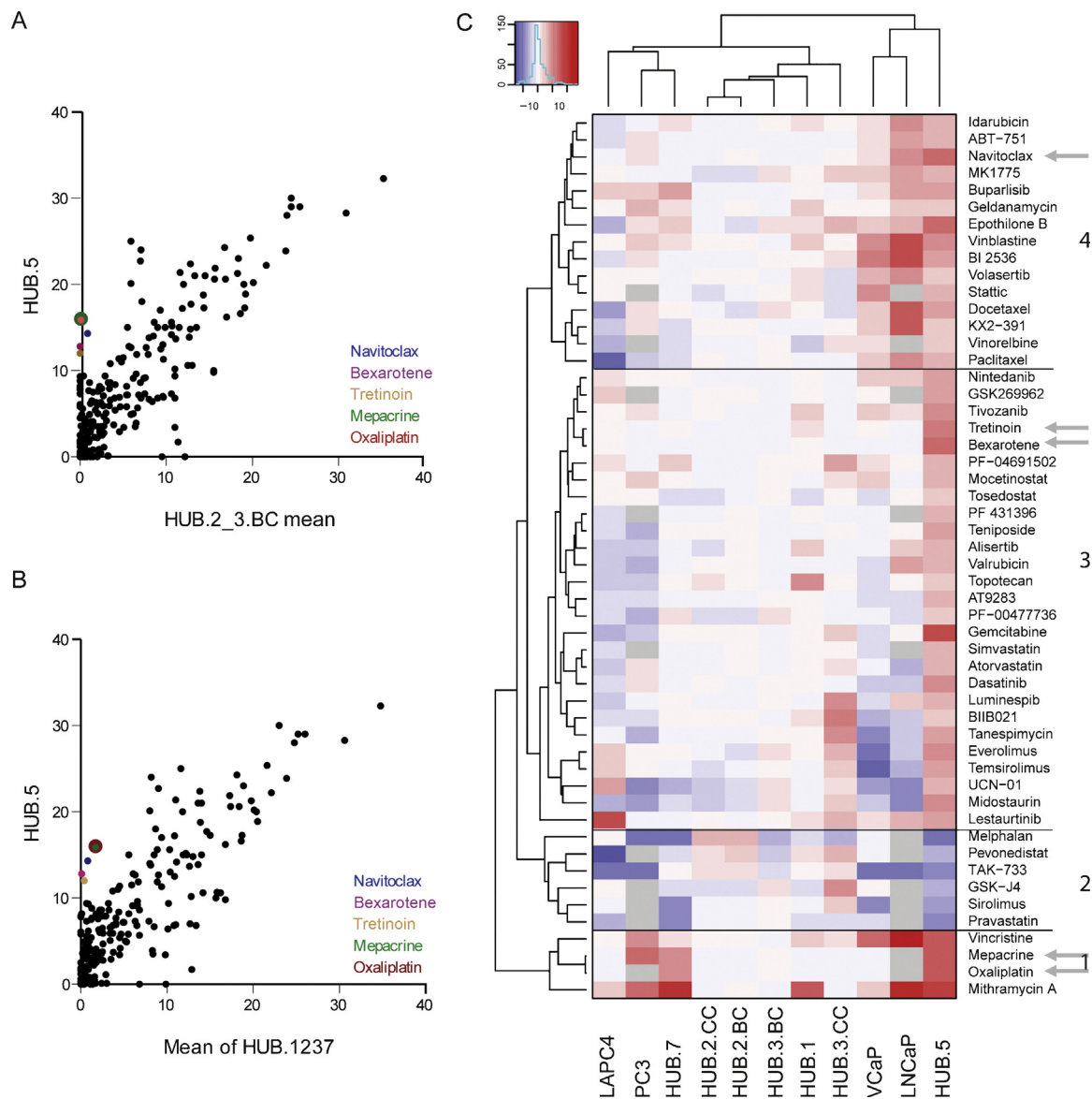


Fig. 3 – Comprehensive drug testing identified sensitivity profiles for the conditionally reprogrammed cells (CRCs). (A) Correlation plot of the drug sensitivity score (DSS) between HUB.5 CRCs (y-axis) and the mean DSS value of two CRCs derived from benign prostate tissue (HUB.2.BC and HUB.3.BC), and (B) mean DSS of all other CRCs (HUB.1–3 and HUB.7) established in this study except for HUB.5 CRCs plotted on the x-axis. (C) Unsupervised hierarchical clustering of patient specific DSS compared with benign controls (HUB.2.BC and HUB.3.BC). Red represents higher DSS or decreased cell viability whereas blue represents lower DSS or higher viability in comparison to the average of two controls. The heat map has been classified into four (1–4 as indicated) distinct patterns based on HUB.5 CRCs' drug responses. The arrows indicate navitoclax, bexarotene, tretinoin, oxaplatin, docetaxel, and mepacrine.

included navitoclax, bexarotene, tretinoin, oxaliplatin, and mepacrine (Fig. 3A and 3B, Supplementary Table 4).

Unsupervised hierarchical clustering was applied to compare the overall drug response profile of the HUB.5 CRCs with all the other CRCs, as well as to the commonly used Pca cell lines LNCaP, LAPC4, PC3, and VCaP (Fig. 3C). Altogether, 46 drugs were more effective in HUB.5 CRCs than the mean of the controls and six drugs showed lower efficacy (Supplementary Table 4B). HUB.5 CRCs clustered together with the Pca cell lines VCaP and LNCaP, whereas the other CRCs formed a distinct cluster. Of the drugs highlighted, oxaliplatin and docetaxel as well as mepacrine

(an antimalaria drug) have been tested in clinical trials for CRPC (clinicaltrials.gov; NCT00260611, NCT01487720, NCT00417274). Gemcitabine also showed high efficacy in HUB.5 CRCs (cluster 3) and the combination of gemcitabine with oxaliplatin has been suggested as a second-line treatment option for metastatic CRPC after failure of docetaxel [21]. Interestingly, docetaxel and paclitaxel are found in cluster 4 along with navitoclax, which was the most effective targeted drug and the most specific for HUB.5 CRCs (Fig. 3A and 3B, Supplementary Table 4). Navitoclax in combination with abiraterone is currently undergoing phase II trials for metastatic CRPC (NCT01828476).

3.4. Navitoclax induces apoptosis in CRPC-derived HUB.5 CRCs

RNA sequencing data indicated elevated expression of Bcl-2 family members Bcl-xL and Mcl-1 in both HUB.5 tumor tissue and CRCs (Fig. 4A). These findings were validated using quantitative polymerase chain reaction and IHC for Bcl-xL

and Mcl-1 (Fig. 4B and 4C). To validate the navitoclax sensitivity of HUB.5 CRCs, we quantified the apoptotic cells by the expression of cleaved Caspase-3 under navitoclax exposure using IF labeling and supervised machine learning image analysis. These results show an increase in cleaved Caspase-3-positive cells after 24–72 h of navitoclax

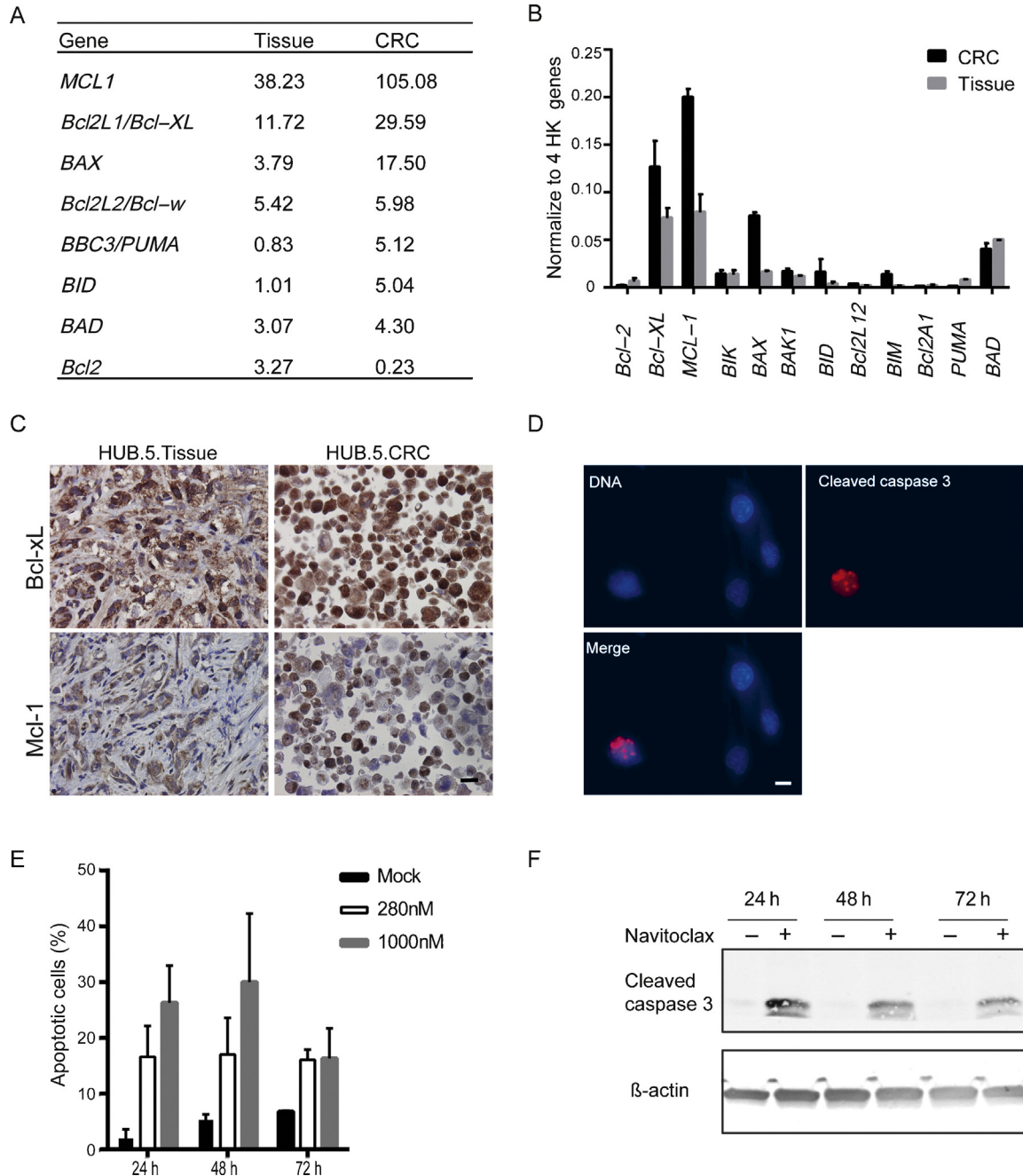


Fig. 4 – The expression of Bcl-2 family members and impact of navitoclax in castration-resistant prostate cancer derived conditionally reprogrammed cells (CRCs). (A) RNA sequencing results of the Bcl-2 family members in HUB.5 tissue and CRCs presented in fragments per kilobase of exon per million fragments mapped values. (B) Real-time quantitative reverse transcription polymerase chain reaction analysis of the Bcl-2 family members to verify RNA sequencing data. The expression was normalized to the average of four housekeeping (HK) genes (*18S ribosomal RNA*, *B2 M*, *RPLP0*, and *ACTB*). Error bars are representing the \pm standard deviation of two independent technical replicate experiments. (C) Immunohistochemistry staining of Bcl-xL and Mcl-1 in HUB.5 tissue and CRCs. The representative images were obtained using 40 \times objective and the scale bar indicates 20 μ m. (D) A representative image showing the HUB.5 response to navitoclax. Red immunofluorescence staining indicates the cleavage of Caspase-3 in HUB.5 CRCs after 24 h exposure to navitoclax (280 nM). Blue color indicates nuclei stained with Hoechst 33342. The images were obtained using 40 \times objective and the scale bar indicates 10 μ m. (E) Quantification of the apoptotic cells (as shown in D) by cCaspase-3 and DNA labeling. A total of 376 to 776 cells were analyzed per sample. (F) Western blotting analysis of cCaspase-3 and actin as a loading control in HUB.5 CRCs after 24 h, 48 h, and 72 h of navitoclax (280 nM) exposure. Dimethyl sulfoxide was used as control vehicle in D and F.

treatment compared with mock treated cells (Fig. 4D and 4E). Similarly, western blotting analysis validated the apoptotic response of navitoclax showing cleavage of caspase-3 only in HUB.5 CRCs (Fig. 4F), and not in two other CRCs (HUB.1 and HUB.3.CC) which were also resistant to navitoclax in the primary testing (Supplementary Fig. 4A and 4B). Together, these results show that navitoclax, initially identified through drug testing, is effective in inducing apoptosis in the CRPC-derived HUB.5 CRCs. HUB.5 CRCs' sensitivity to navitoclax is consistent with the protein expression profile showing increased expression of Bcl-2 family members Bcl-xL and Mcl-1 (Fig. 4C).

4. Discussion

We had almost 80% success in establishing ex vivo CRC cultures from prostate tissues, including one CRC culture with a clonal relationship to the original tumor tissue was established from a patient with CRPC (HUB.5). The patient with a more clinically aggressive disease (HUB.5) had a relatively homogenous cancer content with no benign cells present in the parental tissue specimen. This sample gave rise to CRCs presenting shared CNAs with the parental tissue, while most other PCa samples gave rise to genomically normal, likely benign cell cultures.

The majority of the CRCs were identified as TA, which is in agreement with the presumed cell type that acts as a prostate progenitor [22]. TA cells are androgen-independent and do not express AR or PSA, but this phenotype is transitory and the cells differentiate to express luminal markers in appropriate growth conditions. AR and PSA negative cancer cells have been suggested to exhibit long-term tumor-propagating capacity, and they are refractory to androgen deprivation and consequently evade apoptosis during treatment [15]. Moreover, these types of cells have been suggested to repopulate the tumors after antiandrogen treatment. Similarly, high expression of the prosurvival Bcl-2 family members (Bcl-2 and Bcl-xL) is frequent in advanced PCa and has been linked to drug resistance [23]. Therefore, targeting the expression of Bcl-2 family members, for example, Bcl-2, Bcl-xL, Bcl-W, and Mcl-1, could sensitize cells to chemotherapy [23–25]. The comprehensive drug testing identified several clinical and emerging drugs showing selective efficacy against the CRPC-derived HUB.5 CRCs (Fig. 3). Importantly, we were able to find efficacies for nonhormonal drugs such as taxanes, which are commonly used in clinical practice, as well as less well-established anti-PCa drugs such as mepacrine, oxaliplatin, and navitoclax, many of which are also currently undergoing clinical trials in different combinations for CRPC. Indeed, the drug sensitivity profile identified for HUB.5 CRCs—the CRPC culture established in this study—provides both validation of the efficacy of existing and emerging anti-PCa drugs as well as generates starting points for new drug repositioning efforts in CRPC. Thus, our approach to combine novel methods for culturing PCa primary cells with high-throughput drug testing technology provides insights for drug development, drug repositioning, and possibly in the future, precision oncology.

5. Conclusions

Better functional understanding of cell signaling and drug vulnerabilities in clinical human PCa tissues is urgently required to enable therapeutic discoveries. This study provides proof of concept for establishing CRCs from CRPC patients. Drug sensitivity testing of these CRPC-derived CRCs highlighted sensitivity to several potential oncology drugs such as taxanes, mepacrine, oxaliplatin, and navitoclax. The most potent effects were seen with navitoclax, which was linked to the overexpression of Bcl-2 family members and induction of apoptosis.

Author contributions: Taija M. af Hällström had full access to all data in the study and takes responsibility for the integrity of the data and the accuracy of the data analysis.

Study concept and design: Kallioniemi, Östling, af Hällström.

Acquisition of data: Saeed, Rahkama, Eldfors, Bychkov, Mpindi, Yadav, Paavolainen, af Hällström.

Analysis and interpretation of data: Saeed, Rahkama, Eldfors, Bychkov, Mpindi, Yadav, Paavolainen, Horvath, Kallioniemi, Östling, af Hällström.

Drafting of the manuscript: Saeed, Rahkama, Kallioniemi, Östling, af Hällström.

Critical revision of the manuscript for important intellectual content: Saeed, Rahkama, Eldfors, Bychkov, Mpindi, Paavolainen, Aittokallio, Wennerberg, Heckman, Peehl, Mirtti, Rannikko, Kallioniemi, Östling, af Hällström.

Statistical analysis: Eldfors, Yadav, Mpindi, Aittokallio.

Obtaining funding: Saeed, Rannikko, Horvath, Heckman, Kallioniemi, af Hällström.

Administrative, technical, or material support: Östling, Wennerberg, Heckman, Mirtti, Rannikko.

Supervision: Kallioniemi, Östling, af Hällström.

Other: None.

Financial disclosures: Taija M. af Hällström certifies that all conflicts of interest, including specific financial interests and relationships and affiliations relevant to the subject matter or materials discussed in the manuscript (eg, employment/affiliation, grants or funding, consultancies, honoraria, stock ownership or options, expert testimony, royalties, or patents filed, received, or pending), are the following: Kallioniemi is a founder of bioinformatics startup Medisapiens, and recipient of research funding from Pfizer and Roche for studies of nonurological tumors. Heckman receives research support from Celgene for hematological analyses. The Institute for Molecular Medicine Finland has a collaboration agreement with Labcyte Inc. about liquid dispensing for high-throughput drug testing.

Funding/Support and role of the sponsor: The research leading to these results has received funding from the European Union's Seventh Framework Programme (FP7/2007–2013) under grant agreement number 258068; EU-FP7-Systems Microscopy NoE, Sigrid Juselius Foundation, Cancer Society of Finland, Academy of Finland, the Magnus Ehrmrooth foundation and TEKES FiDiPro Fellow Grant 40294/13, and TEKES new generation biobanking grant 40294/11.

Acknowledgments: We would like to thank Vilja Pietiäinen, Mariliina Arjama, Dishaben Malani, Tanja Ruokoranta, and Piia Mikkonen from the Kallioniemi Research Group; Tiina Vesterinen, Kimmo Pitkänen, Siv Knaappila, Reija Randen-Brady, and Arja Tapio from the Helsinki Urological Biobank Project; Swapnil Potdar, Laura Turunen, Matti Kankainen, and Jani Saarela from the FIMM High Throughput Biomedicine Unit; Alun Parsons from the Heckman Research Group; Pirkko

Mattila and Pekka Ellonen from the FIMM Sequencing Unit; and Biomedicum Imaging unit for excellent technical assistance. We would also like to thank Helsinki Urological Biobank patients for participating in this study.

Appendix A. Supplementary data

Supplementary data associated with this article can be found, in the online version, at <http://dx.doi.org/10.1016/j.eururo.2016.04.019>.

References

- [1] Heidenreich A, Bastian PJ, Bellmunt J, et al. EAU guidelines on prostate cancer. Part II: Treatment of advanced, relapsing, and castration-resistant prostate cancer. *Eur Urol* 2014;65:467–79.
- [2] Heidenreich A, Bastian PJ, Bellmunt J, et al. EAU guidelines on prostate cancer. part 1: screening, diagnosis, and local treatment with curative intent-update 2013. *Eur Urol* 2014;65:124–37.
- [3] Pagliarulo V, Bracarda S, Eisenberger MA, et al. Contemporary role of androgen deprivation therapy for prostate cancer. *Eur Urol* 2012;61:11–25.
- [4] Montgomery RB, Mostaghel EA, Vessella R, et al. Maintenance of intratumoral androgens in metastatic prostate cancer: a mechanism for castration-resistant tumor growth. *Cancer Res* 2008;68:4447–54.
- [5] de Bono JS, Logothetis CJ, Molina A, et al. Abiraterone and increased survival in metastatic prostate cancer. *N Engl J Med* 2011;364:1995–2005.
- [6] Scher HI, Fizazi K, Saad F, et al. Increased survival with enzalutamide in prostate cancer after chemotherapy. *N Engl J Med* 2012;367:1187–97.
- [7] Tannock IF, de Wit R, Berry WR, et al. Docetaxel plus prednisone or mitoxantrone plus prednisone for advanced prostate cancer. *N Engl J Med* 2004;351:1502–12.
- [8] de Bono JS, Oudard S, Ozguroglu M, et al. Prednisone plus cabazitaxel or mitoxantrone for metastatic castration-resistant prostate cancer progressing after docetaxel treatment: a randomised open-label trial. *Lancet* 2010;376:1147–54.
- [9] Heidenreich A, Scholz HJ, Rogenhofer S, et al. Cabazitaxel plus prednisone for metastatic castration-resistant prostate cancer progressing after docetaxel: results from the German compassionate-use programme. *Eur Urol* 2013;63:977–82.
- [10] Schrader AJ, Boegemann M, Ohlmann CH, et al. Enzalutamide in castration-resistant prostate cancer patients progressing after docetaxel and abiraterone. *Eur Urol* 2014;65:30–6.
- [11] Parker C, Nilsson S, Heinrich D, et al. Alpha emitter radium-223 and survival in metastatic prostate cancer. *N Engl J Med* 2013;369:213–23.
- [12] Uzgare AR, Xu Y, Isaacs JT. In vitro culturing and characteristics of transit amplifying epithelial cells from human prostate tissue. *J Cell Biochem* 2004;91:196–205.
- [13] van Leenders GJ, Schalken JA. Epithelial cell differentiation in the human prostate epithelium: implications for the pathogenesis and therapy of prostate cancer. *Crit Rev Oncol Hematol* 2003;46(Suppl):S3–10.
- [14] Bonkhoff H, Remberger K. Differentiation pathways and histogenetic aspects of normal and abnormal prostatic growth: a stem cell model. *Prostate* 1996;28:98–106.
- [15] Qin J, Liu X, Laffin B, et al. The PSA(-/lo) prostate cancer cell population harbors self-renewing long-term tumor-propagating cells that resist castration. *Cell Stem Cell* 2012;10:556–69.
- [16] Liu X, Ory V, Chapman S, et al. ROCK inhibitor and feeder cells induce the conditional reprogramming of epithelial cells. *Am J Pathol* 2012;180:599–607.
- [17] Chua CW, Shibata M, Lei M, et al. Single luminal epithelial progenitors can generate prostate organoids in culture. *Nat Cell Biol* 2014;16:951–61.
- [18] Gao D, Vela I, Sboner A, et al. Organoid cultures derived from patients with advanced prostate cancer. *Cell* 2014;159:176–87.
- [19] Pemovska T, Kontro M, Yadav B, et al. Individualized systems medicine strategy to tailor treatments for patients with chemorefractory acute myeloid leukemia. *Cancer Discov* 2013;3:1416–29.
- [20] Yadav B, Pemovska T, Szwajda A, et al. Quantitative scoring of differential drug sensitivity for individually optimized anticancer therapies. *Sci Rep* 2014;4:5193.
- [21] Lee JL, Ahn JH, Choi MK, et al. Gemcitabine-oxaliplatin plus prednisolone is active in patients with castration-resistant prostate cancer for whom docetaxel-based chemotherapy failed. *Br J Cancer* 2014;110:2472–8.
- [22] Supryniewicz FA, Upadhyay G, Krawczyk E, et al. Conditionally reprogrammed cells represent a stem-like state of adult epithelial cells. *Proc Natl Acad Sci U S A* 2012;109:20035–40.
- [23] Lebedeva I, Rando R, Ojwang J, Cossum P, Stein CA. Bcl-xL in prostate cancer cells: effects of overexpression and down-regulation on chemosensitivity. *Cancer Res* 2000;60:6052–60.
- [24] Krajewska M, Krajewski S, Epstein JI, et al. Immunohistochemical analysis of bcl-2, bax, bcl-X, and mcl-1 expression in prostate cancers. *Am J Pathol* 1996;148:1567–76.
- [25] Stackhouse GB, Sesterhenn IA, Bauer JJ, et al. p53 and bcl-2 immunohistochemistry in pretreatment prostate needle biopsies to predict recurrence of prostate cancer after radical prostatectomy. *J Urol* 1999;162:2040–5.